Wirths, Heiko; Rathmann, Joachim; Michaelis, Peter

Working Paper

Climate feedbacks in DICE-2013R: Modeling and empirical results

Volkswirtschaftliche Diskussionsreihe, No. 327

Provided in Cooperation with:
University of Augsburg, Institute for Economics

Suggested Citation: Wirths, Heiko; Rathmann, Joachim; Michaelis, Peter (2016) : Climate feedbacks in DICE-2013R: Modeling and empirical results, Volkswirtschaftliche Diskussionsreihe, No. 327, Universität Augsburg, Institut für Volkswirtschaftslehre, Augsburg

This Version is available at:
http://hdl.handle.net/10419/155640

Institut für Volkswirtschaftslehre

Volkswirtschaftliche Diskussionsreihe

Climate Feedbacks in DICE-2013R
Modeling and Empirical Results

Heiko Wirths, Joachim Rathmann, Peter Michaelis

Beitrag Nr. 327, Juli 2016

Climate Feedbacks in DICE-2013R

Modeling and Empirical Results

Heiko Wirths Joachim Rathmann Peter Michaelis

Abstract: Climate feedback mechanisms that have the potential to intensify global warming have been omitted almost completely in the integrated assessment of climate change and the economy so far. With the present paper we try to narrow this gap in literature. We discuss different types of feedback mechanisms and show how to incorporate them into the mathematical setup of the well-known integrated assessment model DICE-2013R. Subsequently, we choose the permafrost carbon feedback (PCF) as specific application for an empirical analysis. We calibrate the parameters for our modified version of the DICE-2013R model and compute the optimal emission mitigation rates that maximize welfare accounting for the impact of the PCF. Finally, we quantify the economic losses resulting from a mitigation policy which ignores this feedback mechanism. Our empirical results generally indicate that accounting for the PCF leads to an increase in the optimal mitigation rates.

Keywords: integrated assessment, DICE model, climate feedbacks, permafrost.

JEL: O44, Q54, Q58.

H. Wirths (corresponding author), Faculty of Business and Economics, University of Augsburg, Universitaetsstrasse 16, D-86159 Augsburg, Germany.
E-Mail: heiko.wirths@wiwi.uni-augsburg.de.

J. Rathmann, Faculty of Applied Computer Science, Institute of Geography, University of Augsburg, Germany.

P. Michaelis, Faculty of Business and Economics, University of Augsburg, Germany.

1 Introduction

Although the direct effects of greenhouse gases on global temperature are relatively well understood, estimation of the overall effects is complicated due to the existence of feedback mechanisms in the climate system that have the potential to intensify global warming (e.g., Wolff et al. 2015). Higher temperatures, for instance, may lead to an increased release of CO_2 and CH_4 from permafrost regions that in turn accelerates the increase in temperature. Such mechanisms have been omitted almost completely in the integrated assessment of climate change and the economy so far.[1] This paper shows how to incorporate climate feedbacks into the mathematical setup of the well-known integrated assessment model DICE-2013R (see Nordhaus 2013) and derives some empirical results.

Integrated assessment models (IAMs) are a popular tool when studying the economics of climate change (e.g., Hof et al. 2012). The major components of those IAMs are a neoclassical growth model and a climate module that is linked to the economic model. Important characteristics of those IAMs are their intertemporal formulation and the incorporation of a long time horizon. Since greenhouse gases have a long residence time in the atmosphere (often more than 100 years), this model setup is necessary for a meaningful assessment of climate change. Taking into account the mitigation costs and potential climate damage costs, one major subject of study in IAMs is the economically optimal emission mitigation path. Although we are aware of massive reservations against these models, we do not agree with the part of criticism that climatic feedback loops are "largely unknown" (Pindyck 2013, p. 870). On the contrary, we try to improve the model results by integrating such feedback mechanisms to slightly reduce the simplifications of DICE-2013R.

The use of DICE-2013R for this paper has several reasons. Since the development of the first version of DICE (Nordhaus 1994), it is probably the most popular IAM in the economics of climate change and its codes are publicly available.[2] Due to its popularity, DICE entails the advantage that our results are comparable with those of many other studies using the same model family. This is particularly important since climatic feedbacks are closely related to tipping points[3] and potential catastrophes which have been assessed in a couple of studies within the DICE framework. For example, Mastrandrea and Schneider (2001) and Keller et al. (2004) show that optimal emission mitigation increases when uncertainty and potential catastrophes are included in the DICE-94 model. Ackerman et al. (2010) present a similar analysis for DICE-07, and Rezai (2010) introduces an upper limit for the atmospheric carbon absorption in order to account for potential catastrophes. Moreover, Lemoine and Traeger (2014a) use DICE-07 to analyze the impact of multiple tipping points that reinforce each other's economic impacts.

The paper is organized as follows. In the next section we present those parts of the original DICE-2013R model which are essential for the implementation of climate feedback loops. In

[1] The only exception is a short paper recently published by Gonzáles-Eguino and Neumann (2016) which, however, is more limited in scope than our analysis – see also Section 3.3.

[2] See http://www.econ.yale.edu/~nordhaus/homepage/.

[3] The term "tipping point" refers to critical thresholds that can change the climate system abruptly (see also Section 3).

Section 3 we briefly describe some of the most important feedbacks and show how to incorporate them into the mathematical setup of DICE-2013R. In a subsequent empirical analysis we focus on the permafrost carbon feedback (PCF) because this is one of the most studied and best understood feedback mechanisms. In Section 4 we calibrate the parameters for our modified version of the model, and in Section 5 we discuss our empirical results. Finally, in Section 6 we summarize the paper.

2 The DICE-2013R model

The main components of the model are a neoclassical growth model (Ramsey 1928) that is linked to a climate module which consists of a simple representation of the global carbon cycle.[4] These two components are linked via greenhouse gas emissions that are mainly caused by production. Global warming resulting from these emissions then in turn affects production possibilities which leads to climate damages. The main focus of DICE lies on the trade-off between these damages and costly emission mitigation measures. Hence, solving the model yields the economically optimal mitigation policy.

In the following we refer to the version DICE-2013R (Nordhaus 2013) and present only those equations which are essential concerning the implementation of climate feedback loops. A short summary of the model is available in the Annex. Emissions E(t) are composed of an endogenous component resulting from production activities and an exogenous component resulting from land use changes like deforestation denoted as $E_{def}(t)$:

$$E(t) = \tau(t)[1-\mu(t)]Y(t) + E_{def}(t). \tag{1}$$

The variable Y(t) indicates gross output and $\tau(t)$ is an exogenous emission coefficient which declines over time in order to simulate carbon-saving technological change. Moreover, $\mu(t)$ is the endogenous mitigation rate, i.e., the share of emissions avoided by abatement activities. The remaining emissions according to (1) accumulate in the atmosphere and cause the atmospheric carbon concentration to increase. The latter is interrelated with the concentrations in different layers of the oceans. The concentrations in the atmosphere $M_{AT}(t)$, in the upper ocean $M_{UO}(t)$ and in the lower ocean $M_{LO}(t)$ and their interrelationship are:

$$M_{AT}(t) = E(t) + [1-\phi_{12}]\cdot M_{AT}(t-1) + \phi_{21}\cdot M_{UO}(t-1), \tag{2}$$

$$M_{UO}(t) = \phi_{12}\cdot M_{AT}(t-1) + \phi_{22}\cdot M_{UO}(t-1) + \phi_{32}\cdot M_{LO}(t-1), \tag{3}$$

$$M_{LO}(t) = \phi_{23}\cdot M_{UO}(t-1) + \phi_{33}\cdot M_{LO}(t-1). \tag{4}$$

The atmospheric concentration $M_{AT}(t)$ is composed of the current emissions, the share of the concentration remaining from the previous period plus the share of the upper oceanic concentration from the previous period that diffuses into the atmosphere. The upper oceanic concentration $M_{UO}(t)$ consists of the remaining share from the previous period plus the absorptions from the atmosphere and the lower oceans. The concentration in the lower oceans $M_{LO}(t)$ is

[4] For an extensive description of the model see Nordhaus (2013) and Nordhaus and Sztorc (2013).

the remaining share of the previous period plus the absorption from the upper oceans. The parameters ϕ_{ij} control these relationships between different reservoirs and periods.

In the next step, the atmospheric carbon concentration $M_{AT}(t)$ increases the radiative forcing from the sun F(t) represented by:

$$F(t) = \eta \cdot \frac{M_{AT}(t)}{M_{AT}(preind)} + F_{exog}(t) \tag{5}$$

with η being a parameter that controls the impact of increasing greenhouse gas concentrations and $M_{AT}(preind)$ indicating the pre-industrial level of these concentrations. The term $F_{exog}(t)$ covers the additional radiative forcing caused by other greenhouse gases or aerosols that are exogenous in the model. Finally, the increasing radiative forcing results in an increase of temperatures in the atmosphere $\Delta T_{AT}(t)$ as well as in the oceans $\Delta T_{O}(t)$.[5]

3 Climate feedbacks and their modeling in DICE-2013R

Climate feedback mechanisms as considered in the present paper are processes that have the potential to accelerate global warming.[6] Hence, these mechanisms increase the danger of reaching critical tipping points where earth's climate abruptly moves between relatively stable states. When the system is already close to such a tipping point, even small changes in temperature can have dramatic consequences which are hard to predict. Examples are the melt of the Greenland ice sheet, the shutoff of the Atlantic deep water formation or the collapse of the Indian summer monsoon (Lenton et al. 2008).

Climate feedback mechanisms and tipping points are a relatively new challenge to the modeling of the climate's effect on the economy. Since several recent studies already address tipping points in the context of climate economics (e.g., Lemoine and Traeger 2014a, 2014b) we will focus our analysis on feedback mechanisms. When modeling these mechanisms it is most important to account for their self-enforcing character. For example, melting glaciers lead to an increase in temperature which in turn leads to a further melting of glaciers (see also Section 3.1.1). Modeling such interactions in DICE-2013R requires to identify the corresponding part of the model and to include an appropriate endogenous feedback loop. In the following this is illustrated for some of the most important kinds of climate feedbacks.

3.1 Snow and ice albedo

Albedo is the fraction of the incoming shortwave radiation (solar energy) which is reflected from the earth back into space. Hence, the higher the albedo, the lower is the radiative forcing F(t) described above by equation (5). Snow and ice have a high albedo, whereas water and land surface uncovered by snow or ice have a much lower albedo. Consequently, as snow and ice melts, more of the sun's energy is absorbed. This leads to a further warming which in turn

[5] Strictly speaking, the variables $\Delta T_{AT}(t)$ and $\Delta T_{O}(t)$ represent the difference in temperatures compared to their pre-industrial level.

[6] Additionally, there also exist some so-called negative feedback mechanisms that can slow down global warming (see, e.g., Wolff et al. 2015).

melts even more snow and ice implying a further decrease in albedo. In the following two subsections we consider this feedback loop for glaciers and for the West Antarctic ice shield.

3.1.1 Glacier albedo

Beside sea ice and northern hemispheric snow cover, glaciers have continued to shrink worldwide in recent decades leading to changes in land surface albedo, the hydrological cycle in general and to an increase of the global average sea level. These changes will continue under all RCP[7] scenarios (IPCC 2013). Even high mountain glaciers in the Everest region will probably lose much of their volume, which can be up to a range between 70 and 99% under RCP8.5 conditions by the year 2100 (Shea et al. 2015).

Within the framework of DICE-2013R, the glacier albedo feedback can be incorporated as follows: Due to an increasing atmospheric temperature $\Delta T_{AT}(t)$ glaciers are melting and absorb less radiation; this leads to a higher radiative forcing F(t), which again causes an increase in temperature leading to a further melting of glaciers. Consequently, we propose to include the atmospheric temperature increase $\Delta T_{AT}(t)$ into the equation for radiative forcing (5) as an additional endogenous argument:

$$F(t) = \eta \cdot \frac{M_{AT}(t)}{M_{AT}(\text{preind})} + F_{exog}(t) + \pi_1 \cdot \Delta T_{AT}(t)^{\pi_2} \,. \tag{5a}$$

The additional term $\pi_1 \cdot \Delta T_{AT}(t)^{\pi_2}$ implies that the temperature increase $\Delta T_{AT}(t)$ intensifies the radiative forcing F(t). The extent of this effect caused by melting glaciers can be controlled by the parameters $\pi_1>0$ and $\pi_2>0$. Since an increase in radiative forcing in turn leads to further rising temperatures, equation (5a) constitutes a feedback loop which accelerates global warming.

3.1.2 West Antarctic ice shield

During the last decade the average volume loss of the West Antarctic ice sheet increased by 70% (Paolo et al. 2015).[8] The impact on the radiation budget functions in a pretty similar way as for glaciers. However, concerning the former, the deciding factor is not the atmospheric temperature $\Delta T_{AT}(t)$ but the oceanic temperature $\Delta T_O(t)$ which influences the stability of the ice shield (e.g., Lenton et al. 2008): Higher water temperatures lead to increased melting of the shelf ice which gets thinner. With the shelf becoming thinner, the probability of ruptures increases. The ruptured ice melts in the open sea and thus, the surface of ice (i.e., the area of high radiation reflection) is lost. This loss of ice causes the radiative forcing to increase and ultimately leads to enhanced global warming. To model this feedback, we propose to include the increase of oceanic temperature $\Delta T_O(t)$ into the equation for radiative forcing (5):

---

[7] The abbreviation RCP refers to the four "Representative Concentration Pathways" (RCP2.6, RCP4.5, RCP6, RCP8.5) that are used for climate modeling, describing greenhouse gas concentration trajectories (see van Vuuren et al. 2011). The RCPs define different radiative forcing values (2.6, 4.5, 6.0, 8.5 W/m^2) by the year 2100 relative to pre-industrial values in 1850 and have been used by the IPCC (2013).

[8] However, a complete or nearly complete disintegration of the West Antarctic ice shield is regarded as very unlikely during the 21st century (IPCC 2013).

$$F(t) = \eta \cdot \frac{M_{AT}(t)}{M_{AT}(preind)} + F_{exog}(t) + \varphi_1 \cdot \Delta T_O(t)^{\varphi_2} . \quad (5b)$$

The extension $\varphi_1 \cdot \Delta T_O(t)^{\varphi_2}$ with $\varphi_1>0$ and $\varphi_2>0$ creates a feedback loop similar to the one in section 3.1.1: The increase of the ocean temperature $\Delta T_O(t)$ increases the radiative forcing which leads to higher temperatures.

3.2 Oceanic carbon sink

Oceans can absorb huge amounts of carbon dioxide emissions depending on the atmospheric CO_2 concentration, the ocean water temperature and biological processes which help to transport carbon dioxide into the deep ocean by plankton. As global warming can affect all parts of the atmospheric-ocean carbon exchange chain, long-term projections are difficult. However, it is obvious that the ocean carbon sink is vulnerable to future warming because its uptake capacity is reduced with increasing water temperatures (Arora et al. 2013, Heinze et al. 2015). This implies another feedback loop: With increasing water temperatures the carbon uptake is reduced and more emissions accumulate in the atmosphere enhancing the greenhouse effect. This leads to further warming and further decreasing oceanic carbon uptake. We propose to model this feedback loop as represented by equations (2a) and (3a):

$$M_{AT}(t) = E(t) + \left\lfloor 1 - \frac{\delta_1}{\Delta T_O(t)^{\delta_2}} \cdot \phi_{12} \right\rfloor \cdot M_{AT}(t-1) + \phi_{21} \cdot M_{UO}(t-1) , \quad (2a)$$

$$M_{UO}(t) = \frac{\delta_1}{\Delta T_O(t)^{\delta_2}} \cdot \phi_{12} \cdot M_{AT}(t-1) + \phi_{22} \cdot M_{UO}(t-1) + \phi_{32} \cdot M_{LO}(t-1) . \quad (3a)$$

In the original equations (2) and (3) the parameter ϕ_{12} controls the share of emissions that diffuse from the atmosphere into the upper oceans,[9] and $[1-\phi_{12}]$ is the share that remains in the atmosphere. In the extended equations above this transition effect additionally depends on the ocean temperature change $\Delta T_O(t)$. In equation (3a) the share of emissions absorbed by the upper ocean from the atmosphere is reduced due to the factor $\delta_1 / \Delta T_O(t)^{\delta_2} < 1$. Hence, the share that remains in the atmosphere enlarges as shown in equation (2a). $\delta_1>0$ and $\delta_2>0$ are scaling parameters that control the shape and the strength of this feedback.

3.3 Permafrost

Permafrost is soil (sediment or rock) which remains below 0°C for two or more years and covers about a quarter of the northern hemispheric land surface. Especially in the high-latitude permafrost regions temperatures have risen 0.6°C per decade over the last 30 years, which is twice as fast as the global average (IPCC 2013). Thus, permafrost regions are very sensitive to global climate change. Moreover, in these regions soils have the highest mean soil organic carbon contents. Boreal and Arctic ecosystems contain approximately 50% of global terrestrial organic carbon below ground (Tarnocai et al. 2009). At higher latitudes, these are

[9] The parameter value for ϕ_{12} is 0.088. That means in the original DICE 2013R 8.8% of the atmospheric greenhouse gases are absorbed by the upper oceans within one period (5 years).

frozen over by permafrost, and the embedded greenhouse gases are effectively locked away. However, when the soil thaws due to rising temperatures, the greenhouse gases will become unlocked and be released as CO_2 or CH_4. These additional emissions accumulate in the atmosphere, accelerate global warming and constitute the permafrost carbon feedback (PCF).

Modeling this feedback in DICE-2013R is straightforward: We propose to include the atmospheric temperature increase $\Delta T_{AT}(t)$ as an additional endogenous argument into equation (1) which describes emissions E(t):

$$E(t) = E_{ind}(t) + E_{def}(t) + \varepsilon_1 \cdot \Delta T_{AT}(t)^{\varepsilon_2} . \quad (1a)$$

The extension $\varepsilon_1 \cdot \Delta T_{AT}(t)^{\varepsilon_2}$ in (1a) causes the respective feedback loop: Due to increasing temperatures $\Delta T_{AT}(t)$ the permafrost thaws, depending on the parameters $\varepsilon_1>0$ and $\varepsilon_2>0$. As a result the greenhouse gas accumulation in the atmosphere intensifies which leads to an increase in radiative forcing and further rising temperatures.

Before calibrating the parameters of our model it is necessary to distinguish our analysis from the work recently published by González-Eguino and Neumann (2016). Except for some technical features there are three main differences:

– Firstly, González-Eguino and Neumann (2016) use a carbon budget approach where the temperature increase is handled as an additional restriction and kept below 2 °C. For this constrained scenario the authors calculate the welfare maximizing mitigation rates. In contrast, we follow the original approach of DICE-2013R and calculate the unconstrained welfare maximum. Hence, in our analysis the resulting increase in temperature is completely endogenous.
– Secondly, in the work of González-Eguino and Neumann (2016) emissions from permafrost follow an exogenously given time path, whereas in our analysis PCF-related emissions explicitly depend on temperature thereby constituting an endogenous feedback loop.
– Thirdly, González-Eguino and Neumann (2016) calculate the increase in mitigation rates and the associated cost to society that occur if the 2 °C target has to be met in the presence of emissions from permafrost. In contrast, we also calculate the economic losses resulting from a mitigation policy which ignores the PCF.

4 Calibration of the parameters for the PCF

We chose the PCF for a more throughout empirical investigation within DICE-2013R because the PCF is one of the most studied and best understood climate feedback mechanisms. Several studies have tried to quantify the effect of the PCF on the climate system (e.g., Schneider von Deimling et al. 2012, Schaefer et al. 2014, Koven et al. 2015). Hence, in contrast to the other feedback mechanisms considered in Sections 3.1 and 3.2, we have some more or less reliable data which can be used for calibrating the additional parameters ε_1 and ε_2 in equation (1a).

Following Schneider von Deimling et al. (2012), the extent of the PCF for different RCP emission scenarios is shown in Table 1.[10] These estimates indicate the additional increase in the atmospheric temperature caused by the PCF in the years 2100 and 2200.

Table 1 Additional increase in atmospheric temperature due to the PCF in the years 2100 and 2200 for different RCP emission scenarios (Schneider von Deimling et al. 2012)

	Lower boundary		Best guess		Upper boundary	
	2100	2200	2100	2200	2100	2200
RCP2.6	0.01°C	0.03°C	0.03°C	0.06°C	0.06°C	0.13°C
RCP4.5	0.02°C	0.07°C	0.05°C	0.14°C	0.10°C	0.29°C
RCP6.0	0.02°C	0.10°C	0.05°C	0.20°C	0.11°C	0.46°C
RCP8.5	0.04°C	0.18°C	0.10°C	0.38°C	0.23°C	0.78°C

Schneider von Deimling et al. (2012) studied the PCF within the MAGICC model by Meinshausen et al. (2011a, 2011b). MAGICC is a compact climate model that also has been utilized to calibrate the parameters of the climate module in former versions of the DICE model (Nordhaus 2008, p. 44). For calibrating the parameters ε_1 and ε_2 we use the RCP4.5 scenario because it provides a good match for the respective emissions that are calculated in the standard optimal run of DICE-2013R.

It is important to acknowledge that the values for the RCP4.5 scenario are rather conservative guesses. The RCP6.0 scenario and the RCP8.5 scenario as well as other studies show higher temperature increases as a result of the PCF (e.g., Schaefer et al. 2014). However, we chose the study of Schneider von Deimling et al. (2012) because it provides the best overall assessment considering different RCP scenarios and multiple points in time. Also the authors specified an upper and lower boundary for the temperature increase in each emission scenario.

We calibrated the parameters ε_i by using the extended emission equation according to (1a) but at the same time we fixed the mitigation rates $\mu(t)$ to the values of the standard optimal run of DICE-2013R.[11] This setup was run multiple times resetting the parameters ε_i each time until two requirements were met:

– Firstly, for the best guess as well as for the lower and the upper boundary the additional temperature increase due to the PCF in the years 2100 and 2200 must result exactly in the magnitudes shown for the RCP4.5 scenario in Table 1. Moreover, for the starting year 2010 we require an additional temperature increase of zero which is also roughly in line with the underlying study of Schneider von Deimling et al. (2012).

– Secondly, for all three scenarios the resulting graph concerning the additional temperature increase due to the PCF must exhibit a specific shape: Roughly for the first century the ad-

[10] For an overview on the different RCP emission scenarios and their assumptions see van Vuuren et al. (2011).

[11] All calculations in this paper have been processed with the GAMS-sofware ("General Algebraic Modeling System") using the CONOPT 3 solver. This is the same setup that is used by Nordhaus (2013) for solving the DICE-2013R model. The program file is available from the authors on request.

ditional temperature increase must be more than proportionately, but at some period there must be a turning point such that the increase becomes less than proportionately.

The reason why we require this specific shape is straightforward: When a certain degree of warming is reached, the majority of the permafrost has already thawed and less additional emissions get into the atmosphere. As a result, the effect caused by the PCF diminishes. This is where the turning point occurs and the additional temperature increase becomes less than proportionately.

Table 2 Calibration results for the parameters ε_1 and ε_2 based on the RCP4.5 scenario

	Lower boundary	Best guess	Upper boundary
ε_1	$0.75 \cdot \mathrm{Ord(t)}^{-1}$	$2.55 \cdot \mathrm{Ord(t)}^{-1}$	$5.2 \cdot \mathrm{Ord(t)}^{-1}$
ε_2	$2.9 + 2 \cdot \mathrm{Ord(t)}^{-1}$	$2.35 + 2 \cdot \mathrm{Ord(t)}^{-1}$	$2.35 + 2 \cdot \mathrm{Ord(t)}^{-1}$

The parameters ε_i resulting from our calibration are shown in Table 2 for the best guess scenario as well as the lower and the upper boundary scenario. These expressions look somewhat peculiar due to the variable ord(t) which is part of the GAMS syntax. It simply displays the number of the period that is currently considered (e.g., in period 10 we obtain ord(t)=10). This time-dependent formulation is necessary to meet the estimates by Schneider von Deimling et al. (2012). The reason for this complication is the long residence time of greenhouse gases in the atmosphere which entails that additional emissions due to thawing permafrost take effect for many subsequent periods. Thus, a non-time dependent formulation would always meet either the estimate for 2100 or the estimate for 2200, but never both. In contrast, the time-dependent expressions in Table 2 become smaller over time because ord(t) increases. As a result, the permafrost impact is decreasing. This is also consistent with estimates that most of the emissions due to permafrost thawing will occur roughly up to the year 2150 (Schneider von Deimling et al. 2012).

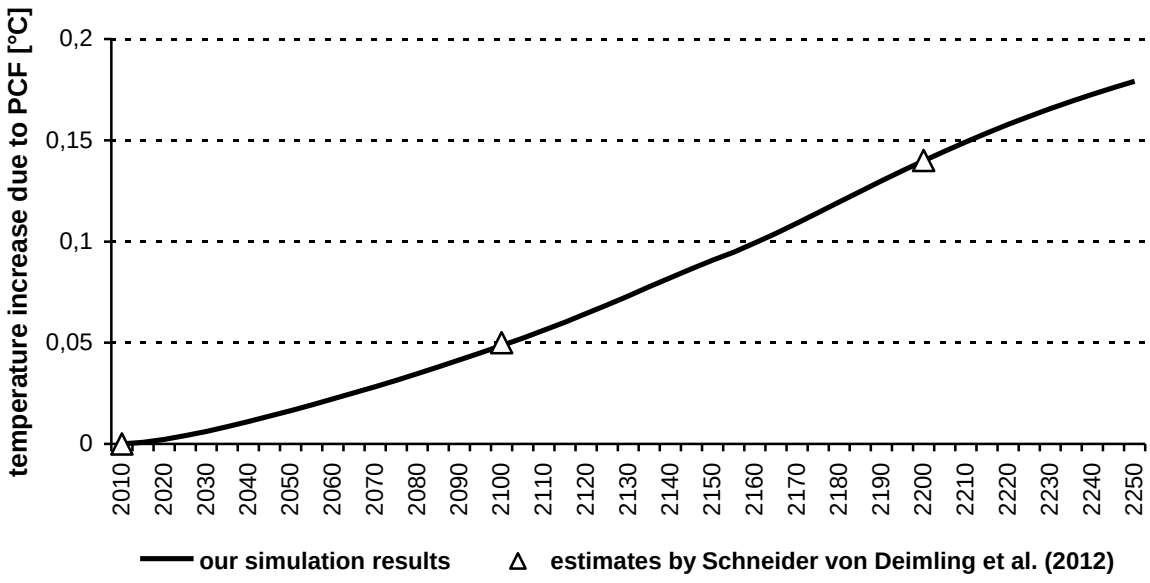

Fig. 1 Temperature increase due to the PCF in the best guess scenario – comparing our simulation results with the estimates of Schneider von Deimling et al. (2012)

Finally, in order to demonstrate the validity of our calibration, Figure 1 shows the additional increase in temperature due to the PCF that results if we employ the parameter values ε_i that stem from our calibration using the best guess scenario. Moreover, the three points marked by the symbol Δ represent the underlying estimates for this scenario by Schneider von Deimling et al. (2012).

5 Results for the PCF

In this section we discuss the results from using the DICE-2013R model with the PCF extension as described above and compare them to the original results of Nordhaus (2013). The major endogenous policy variables are the mitigation rates $\mu(t)$ which describes the share of emissions avoided. Figure 2 shows the "base level" of the mitigation rates resulting from the original DICE-2013R model as calculated by Nordhaus (2013).[12] For the first period (i.e., the year 2010) the mitigation rate is exogenously fixed. The first endogenously optimized mitigation rate occurs in the year 2015 with roughly 20%. From that point on, the mitigation rate rises steadily until it reaches its (temporary) upper limit of 100% in the year 2120. Subsequently, beginning in 2155 the upper limit is relaxed to 120% which causes another jump in Figure 2. Of course, mitigation rates above 100% imply that more emissions are avoided than even occur. This could be interpreted as the employment of some carbon removal techniques which become available by 2155 (e.g., climate engineering).[13]

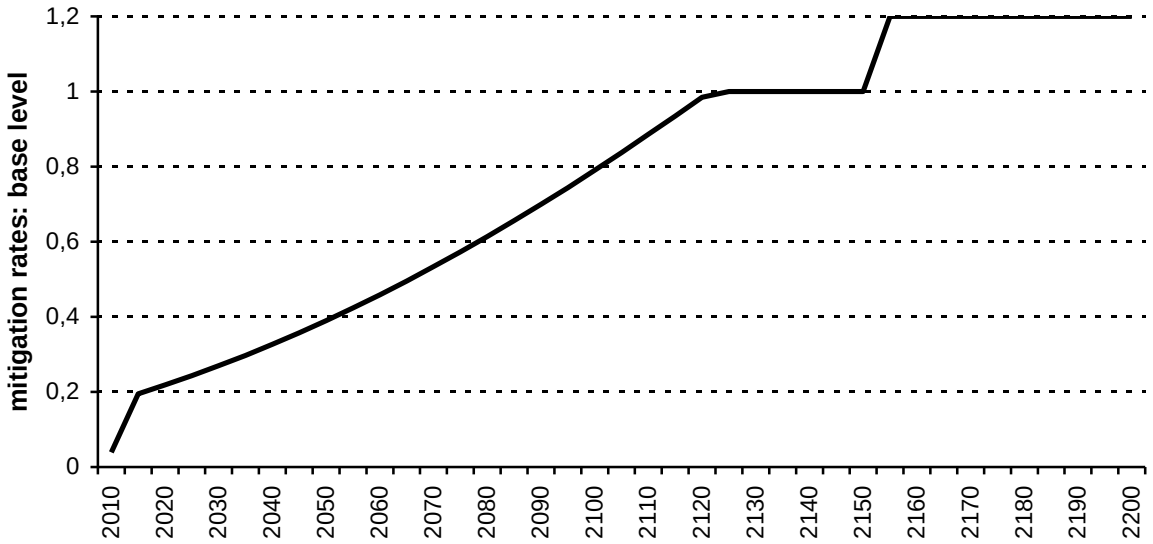

Fig. 2 Optimal mitigation rates in the original DICE-2013R model ("base level")

[12] For convenience, in the text mitigation rates are expressed as percentages although in the original GAMS file as well as in the figures above the variables $\mu(t)$ are expressed as decimals.

[13] However, neither Nordhaus (2013) nor Nordhaus and Sztorc (2013) offer an explicit justification for relaxing the upper limit in 2155.

Next, we present the results of our own calculations using the DICE-2013R model with the PCF extension for the best guess scenario as well as for the upper and the lower boundary.[14] In order to enhance the graphical depiction, Figure 3 does not show the absolute mitigation rates but their *difference* to the base levels as shown in Figure 2. As indicated by Figure 3, in all scenarios the resulting mitigation rates are slightly above the base levels.[15] The reason for this difference is obvious: The PCF leads to increased emissions and therefore to increasing climate damages. Hence, mitigation becomes more favorable.

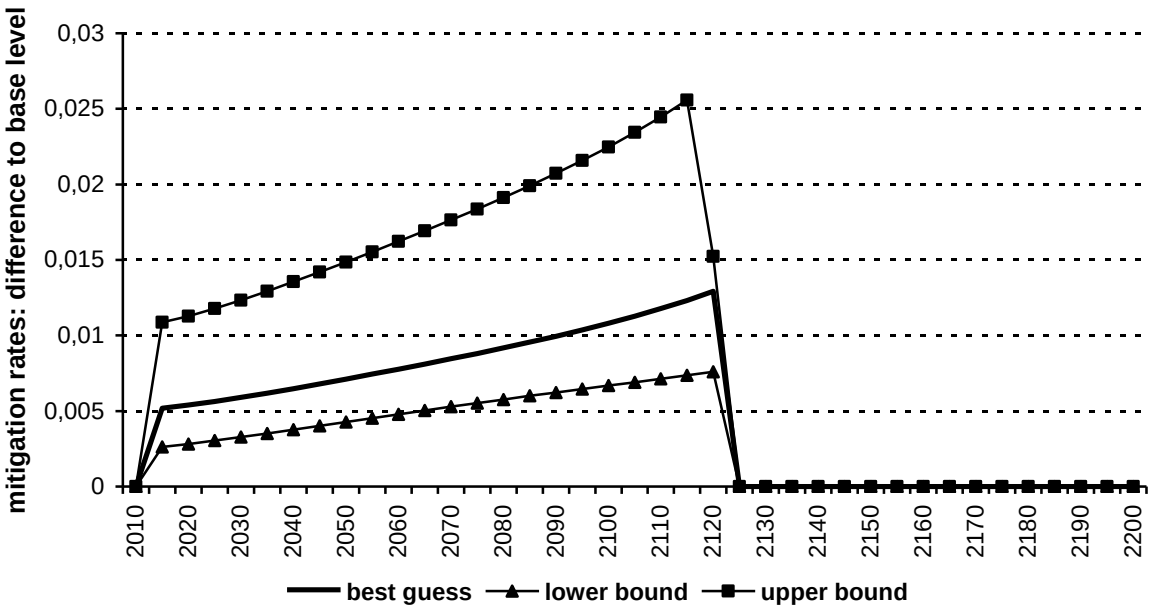

Fig. 3 Difference between optimal mitigation rates with PCF and base level mitigation rates according to Figure 2

For all three scenarios the mitigation rates' differences to the base level increase steadily until they drop down to zero in 2125 since mitigation rates approach to their upper limit in our extended model as well as in the original version. The differences to the base level are biggest in the upper boundary scenario where the PCF is most severe. In this scenario, the differences rise up to roughly 2.7 percentage points. This might seem to be rather small but two crucial points need to be emphasized. Firstly, as already mentioned in Section 4, the magnitudes concerning the PCFs impact on the temperature as shown in Table 1 are quite conservative guesses compared to other studies. And secondly, our model considers only one type of feedback

[14] It should carefully be noted, that the fixation of the mitigation rates $\mu(t)$ to the *base* level in Section 4 was only for the purpose of calibrating the parameters ε_i. The results discussed here, of course, rely on endogenously optimized mitigation rates.

[15] Generally, the PCF-related increase in mitigation rates calculated with our approach is smaller compared to the results obtained by Gonzáles-Eguino and Neumann (2016). The reason is that their model forces the increase in temperature to stay below 2° C whereas unconstrained welfare maximization in our model leads to a peak increase in temperature of about 3.4° C.

mechanism; when multiple feedbacks are considered simultaneously, the overall impact could be expected to be much higher.

Also the differences shown in Figure 3 are small compared to the results of related papers investigating uncertainty and potential catastrophes (Keller et al. 2004, Ackerman et al. 2010). However, these results are only partially comparable. We deal with climate feedbacks that enhance damages but we do not deal with uncertainty about these damages. In contrast, the above cited papers explicitly consider uncertainty leading to much higher emission mitigation rates that can be considered as a risk premium to insure against catastrophes (Nordhaus 2008 pp. 137, Weitzman 2010).

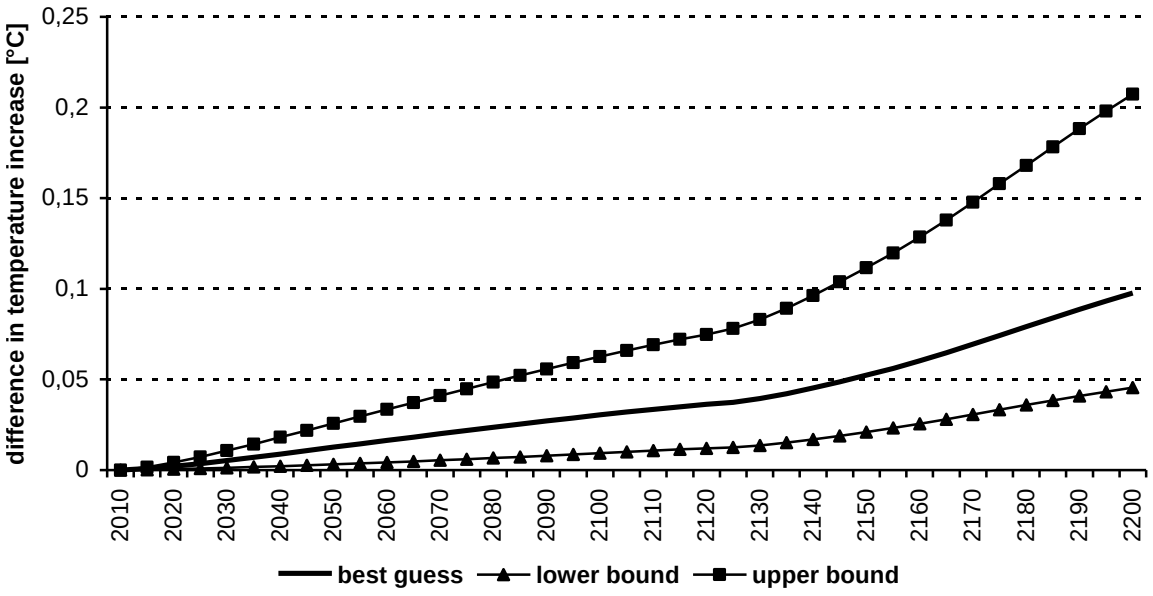

Fig. 4 Temperature increase - difference between our results with optimized mitigation rates and the original DICE2013R model

An important variable directly related to the mitigation rate is the temperature increase. Although our extended model leads to higher mitigation rates compared to Nordhaus (2013) the corresponding atmospheric temperature exceeds the base level resulting from the original version of DICE-2013R. These differences in temperature, as shown in Figure 4, indicate that even in the optimum, enhanced mitigation will only avoid a part of the temperature increase caused by the PCF. However, as easily can be checked, the additional increase in temperature that remains after enhanced mitigation stays well below the reference values for the RCP4.5 scenario presented in Table 1.

Next, in order to investigate potential economic impacts, we compute the output losses that are caused if climate policy ignores that optimal adaption to the PCF requires increasing mitigation rates. Each calculation for the best guess scenario as well as for the upper and the lower boundary proceeds in three steps:

– In the first step, we calculate the output that results if the optimal mitigation rates as derived from our extended model are employed.
– In the second step, the mitigation rates are fixed to the reference values (base level) that stem from the original DICE-2013R without the PCF. Hence, our model is forced to employ suboptimal low mitigation rates. This yields the output that results if climate policy ignores the PCF although its mechanism is present in the model.
– In the third step, the differences in output between the optimal run (first step) and the run with fixed mitigation rates (second step) are calculated. These differences can be interpreted as the economic losses that occur if the PCF is ignored.

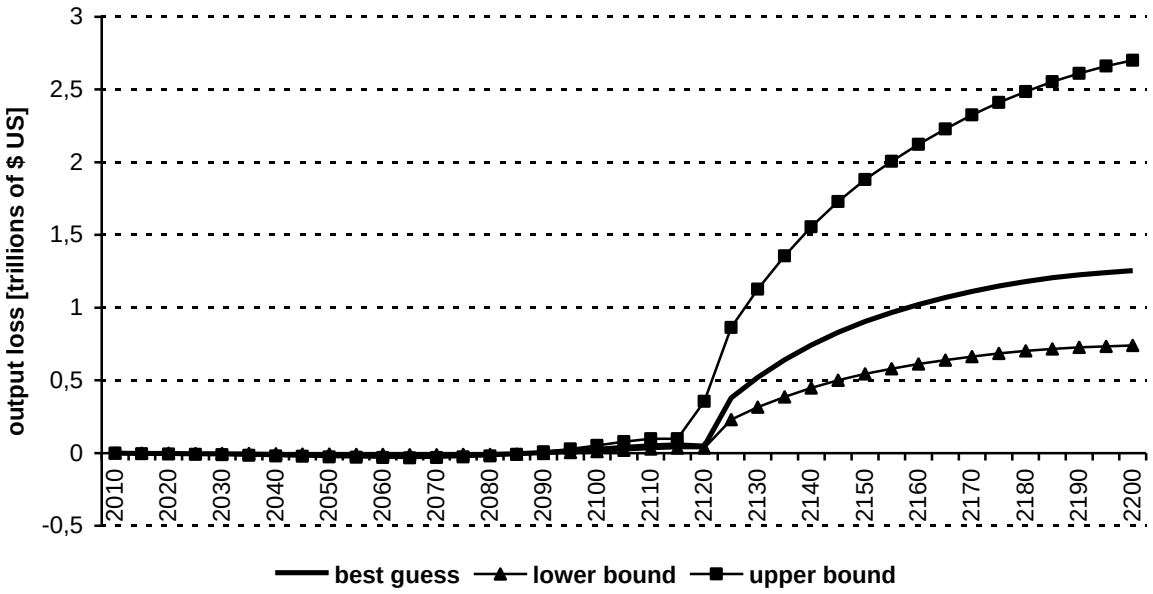

Fig. 5 Output loss that is caused if climate policy ignores the PCF

The undiscounted losses in output (trillions of $ US) resulting from these calculations are shown in Figure 5.[16] Noticeable, the economic impact for roughly the first 100 years is very small since output losses tend to be around zero or even slightly below in all three scenarios. Negative losses imply that actually the suboptimal climate policy with fixed mitigation rates is economically beneficial in those periods. The reason for this is obvious: The optimal climate policy requires higher mitigation rates. This leads immediately to higher mitigation costs, whereas the majority of the benefits in terms of a lower atmospheric carbon concentration accrue in the distant future. Consequently, when considering only the first couple of periods, employing suboptimal low mitigation rates is beneficial.

However, things change drastically by the year 2125 when the graphs suddenly get steeper and output losses become considerably positive. This turn can easily be explained: As indicated by Figure 3, in 2125 the optimal mitigation rates converge to the base level rates shown in Figure 2. Hence, in the following years there are no more additional mitigation costs implied

[16] The same calculations can be performed for the variables consumption and investment. The resulting diagrams are mostly similar to those for output.

by the optimal policy but the economy still profits from the increased mitigation rates in the past.

Finally, we calculated the net present value of output losses employing a pure rate of social time preference of 1,5% as used by Nordhaus (2013). The resulting magnitudes range from 0.9 trillion $ US in the lower boundary scenario, to 1.5 trillion $ US in the best guess scenario and 3.2 trillion $ US in the upper boundary scenario. Compared to the overall net output this implies relative losses ranging from 0.02% to 0.08%. These figures might seem pretty low. However, since the benefits of taking into account the PCF when determining the optimal mitigation rates occur in the distant future, there is an enormous bias caused by discounting. Moreover, as already mentioned above, our results are based on rather conservative estimates of the PCFs impact on temperature.

6 Conclusions

Previous studies on the economics of climate change based on integrated assessment models almost completely omitted the additional effect of feedback mechanisms within the climate system. From the viewpoint of integrated assessment modeling, the most important feature of these mechanisms is their self-enforcing character which leads to endogenous feedback loops. In this paper, we show how to incorporate some of the most important feedback mechanisms into the setup of DICE-2013R. In a subsequent empirical analysis we focus on the PCF which is one of the most studied and best understood climate feedback mechanisms.

Our results showed that maximizing welfare in the presence of an endogenous feedback loop caused by PCF-related emissions requires an increase in mitigation rates that amounts up to 2.7 percentage points (depending on the scenario considered). At first glance, this might seem rather small. However, analyzing multiple feedback mechanisms simultaneously should considerably amplify the impacts illustrated. Moreover, our results are based on rather conservative estimates concerning the impact of the PCF on temperature.

Concerning overall welfare we calculated the economic losses resulting from a mitigation policy which ignores the PCF. It turned out that the main losses occur far in the future when mitigation rates with and without considering the PCF converge such that there are no more additional mitigation costs but the economy would still profit from increased (optimal) mitigation rates in the past. Moreover, this delayed occurrence of losses together with the impact of discounting leads to comparatively small economic effects ranging from -0.02 to -0.08 % when the present value of output is considered.

Of course, we are aware that our analysis can provide only some first insights concerning the incorporation of endogenous feedback loops into integrated assessment models and the resulting economic consequences. Except for the PCF there is still huge uncertainty about the different feedback mechanisms' quantitative impacts on the climate system. Consequently, more studies from the natural sciences are necessary before these mechanisms can be properly calibrated and included into integrated assessment models like DICE.

References

Ackerman F; Stanton EA; Bueno R (2010) Fat tails, exponents, extreme uncertainty: simulating catastrophe in DICE. Ecol Econ 69:1657-1665

Arora VK, Boer GJ, Friedlingstein P, Eby M, Jones CD, Christian JR, Bonan G, Bopp L, Brovkin V, Cadule P, Hajima T, Ilyina T, Lindsay K, Tjiputra JF, Wu T (2013) Carbon–concentration and carbon–climate feedbacks in CMIP5 earth system models. J Climate 26:5289–5314

Gonzáles-Eguino M, Neumann MB (2016) Significant implications of permafrost thawing for climate change control. Clim Change 136:381-388

Heinze C, Meyer S, Goris N, Anderson L, Steinfeldt R, Chang N, Le Quéré C, Bakker DCE (2015) The ocean carbon sink – impacts, vulnerabilities and challenges. Earth Syst Dynam 6:327–358

Hof AF, Hope CW, Lowe J, Mastrandrea MD, Meinshausen M, van Vuuren DP (2010) The benefits of climate change mitigation in integrated assessment models: the role of the carbon cycle and climate component. Clim Change 113:897-917

IPCC (2013) In: TF Stocker, Qin D, GK Plattner, Tignor M, SK Allen, Boschung J, Nauels A, Xia Y, Bex V, PM Midgley (eds) Climate change 2013: the physical science basis. Contribution of working group I to the fifth assessment report of the intergovernmental panel on climate change. Cambridge University Press, Cambridge

Keller K, Bolker BM, Bradford DF (2004), Uncertain climate thresholds and optimal economic growth. J Environ Econ Manag 48:723-741

Koven CD, Schuur EAG, Schädel C, Bohn TJ, Burke EJ, Chen G, Chen X, Ciais P, Grosse G, Harden JW, Hayes DJ, Hugelius G, Jafarov EE, Krinner G, Kuhry P, Lawrence DM, MacDougall AH, Marchenko SS, McGuire AD, Natali SM, Nicolsky DJ, Olefeldt D, Peng S, Romanovsky VE, Schaefer KM, Strauss J, Treat CC, Turetsky M (2015) A simplified, data-constrained approach to estimate the permafrost carbon–climate feedback. Philos T R Soc A 373:20140423

Lemoine D, Traeger CP (2014a) Watch your step: optimal policy in a tipping climate. American Economic Journal: Economic Policy 6:137-166

Lemoine, D, Traeger CP (2014b) Playing the climate dominoes: tipping points and the cost of delaying policy." Working paper, Department of Agricultural and Resource Economics, University of California, Berkley. https://are.berkeley.edu/~traeger/pdf/Lemoine%20Traeger_Tipping%20Domino.pdf. Accessed 19 May 2016

Lenton TM, Held H, Kriegler E, Hall JW, Lucht W, Rahmstorf S, Schellnhuber HJ (2008) Tipping elements in the Earth's climate system. P Natl Acad Sci USA 105:1786-1793

Mastrandrea MD, Michael D, Schneider SH (2001) Integrated assessment of abrupt climate changes. Clim Policy 1:433-449

Meinshausen M, Raper SCB, Wigley TML (2011a) Emulating coupled atmosphere-ocean and carbon cycle models with a simpler model, MAGICC6 - Part 1: Model description and calibration. Atmos Chem Phys 11:1417–1456

Meinshausen M, Raper SCB, Wigley TML (2011b) Emulating atmosphere-ocean and carbon cycle models with a simpler model, MAGICC6 - Part 2: applications. Atmos Chem Phys 11:1457–1471

Nordhaus WD (1994) Managing the global commons. The MIT Press, Cambridge, Mass.

Nordhaus WD (2008) A question of balance: weighing the options on global warming policies, Yale Univ. Press, New Haven

Nordhaus WD (2013), The climate Casino Risk, Uncertainty and Economics for a Warming World, Yale Univ. Press, New Haven

Nordhaus WD, Sztorc P (2013) DICE 2013R: introduction and user's manual. Second edition. http://www.econ.yale.edu/~nordhaus/homepage/documents/DICE_Manual_103113r2.pdf. Accessed 19 May 2016

Paolo FS, Fricker HA, Padman L (2015) Volume loss from Antarctic ice shelves is accelerating. Science: doi:10.1126/science.aaa0940

Pindyck RS (2013) Climate change policy: what do the models tell us? J Econ Lit 51:860–872

Ramsey F (1928) A mathematical theory of saving. Econ J 38:543-559

Rezai A (2010) Recast the DICE and its policy recommendations. Macroecon Dyn 14:275-289

Schaefer K, Lantuit H, Romanovsky VE, Schuur EAG, Witt R (2014) The impact of the permafrost carbon feedback on global climate. Environ Res Lett 9:085003

Schneider von Deimling T, Meinshausen M, Levermann A, Huber V, Frieler K, Lawrence DM, Brovkin V (2012) Estimating the near-surface permafrost-carbon feedback on global warming. Biogeosciences 9:649–665

Shea JM, Immerzeel WW, Wagnon P, Vincent C, Bajracharya S (2015) Modeling glacier change in the Everest region, Nepal Himalaya. The Cryosphere 9:1105–1128

Tarnocai C, Canadell JG, Schuur EAG, Kuhry P, Mazhitova G, Zimov S (2009) Soil organic carbon pools in the northern circumpolar permafrost region. Glob Biogeochem Cycles 23:GB2023

van Vuuren DP, Edmonds J, Kainuma MLT, Riahi K, Thomson A, Matsui T, Hurtt G, Lamarque JF, Meinshausen M, Smith S, Grainer C, Rose S, Hibbard KA, Nakicenovic N, Krey V, Kram T (2011) The representative concentration pathways: an overwiev. Clim Change 109: 5-31

Weitzman ML (2010) GHG Targets as insurance against catastrophic climate damages. Journal of Public Economic Theory 14:221-244

Wolff EW, Shepherd JG, Shuckburgh E, Watson AJ (2015) Feedbacks on climate in the Earth system: introduction. Philos T Roy Soc S-A 373:20140428

Annex

Short description of the DICE-2013R model

The utility in DICE is expressed as a standard constant-relative-risk-aversion utility function for neoclassical growth models:

$$U[c(t), L(t)] = L(t)\left[\frac{c(t)^{1-\alpha}}{1-\alpha}\right] \tag{1}$$

with t indicating the specific period (one period accounts for five years), c(t) is per capita consumption, L(t) is the population and α is the elasticity of marginal utility of consumption. The objective is to maximize the welfare function W. The latter consists of the discounted utility summed over a finite time horizon:

$$W[c(t), L(t)] = \sum_{t=1}^{T} \frac{1}{(1+\rho)^{t-1}} U[c(t), L(t)]. \tag{2}$$

The parameter ρ is the pure rate of social time preference such that $1/(1+\rho)^{t-1}$ is the discount factor. The production function is of Cobb-Douglas type:

$$Y(t) = A(t)K(t)^{\gamma} L(t)^{1-\gamma}. \tag{3}$$

A(t) is the total factor productivity, K(t) is the capital stock, L(t) is not only the population but also the labor input and γ is the elasticity of output with respect to capital. The link to the climate module is formed via greenhouse gas emissions which are caused by production due to an exogenous emission coefficient (see also equation (7)). These emissions accumulate in the atmosphere. The carbon dioxide concentrations in the atmosphere and in the oceans are interrelated, since oceans are considered a huge sink for emissions (Nordhaus 2008 p. 43). As described below by equations (9) to (14), the accumulated emissions lead to a higher atmospheric greenhouse gas concentration which causes the radiative forcing to increase and ultimately cause the surface temperature to increase. The impact of this temperature increase is given by the following damage function Ω(t) which indicates the share of output that is lost due to climate damages:

$$\Omega(t) = \sigma_1 \cdot \Delta T_{AT}(t) + \sigma_2 \cdot \Delta T_{AT}(t)^2. \tag{4}$$

$\Delta T_{AT}(t)$ is the increase of global mean temperature of the atmosphere over the pre-industrial level, and σ_1 as well as σ_2 are parameters that determine the shape of the damage function. To avoid damages, emissions can be reduced by mitigation activities. The accompanying costs Λ(t) are expressed as the share of output that is lost due to mitigation activities. The cost function describing Λ(t) is given by:

$$\Lambda(t) = \psi_1 \cdot \mu(t)^{\psi_2} \tag{5}$$

with $\mu(t)$ indicating the share of avoided emissions, and ψ_1 as well as ψ_2 are parameters that determine the shape of the mitigation cost function.

To sum up, $\Omega(t)$ indicates the share of output lost due to climate damages, whereas $\Lambda(t)$ indicates the share of output lost due to mitigation activities. Consequently, weighting the gross output $Y(t)$ by the multipliers $[1-\Omega(t)]$ and $[1-\Lambda(t)]$ yields the remaining net output:

$$Y_{net}(t) = [1-\Omega(t)][1-\Lambda(t)]A(t)K(t)^{\gamma}L(t)^{1-\gamma}. \tag{6}$$

Equation (6) highlights the typical trade-off in climate policy: More emission mitigation leads to higher mitigation costs $\Lambda(t)$ resulting in a decreasing net output. However, at the same time, more emission mitigation leads to lower damages $\Omega(t)$ resulting in an increasing net output.

Finally, the net output is divided into consumption and investment: $Y_{net}(t) = C(t) + I(t)$. This creates the typical trade-off in neoclassical growth models. Output is either consumed directly or invested in physical capital in order to increase the consumption possibilities in the future.

Emissions are caused by production depending on an exogenous emission coefficient $\tau(t)$ which declines over time in order to simulate carbon-saving technological change. Accounting for abatement activities, the remaining emissions from production are given by:

$$E_{ind}(t) = \tau(t)[1-\mu(t)]A(t)K(t)^{\gamma}L(t)^{1-\gamma} \tag{7}$$

with $\mu(t)$ indicating the mitigation rate, i.e., the share of emissions avoided. Besides emissions from production the model also accounts for exogenously given emissions from land use changes (e.g., deforestation) which are denoted by $E_{def}(t)$. Hence, the complete emissions are given by:

$$E(t) = E_{ind}(t) + E_{def}(t). \tag{8}$$

These emissions accumulate in the atmosphere and cause the atmospheric carbon concentration to increase. The latter is interrelated with the concentrations in different layers of the oceans. The concentrations in the atmosphere $M_{AT}(t)$, in the upper ocean $M_{UO}(t)$ and in the lower ocean $M_{LO}(t)$ and their interrelationship are shown in equations (9) to (11):

$$M_{AT}(t) = E(t) + \left[1-\phi_{12}\right]\cdot M_{AT}(t-1) + \phi_{21}\cdot M_{UO}(t-1), \tag{9}$$

$$M_{UO}(t) = \phi_{12}\cdot M_{AT}(t-1) + \phi_{22}\cdot M_{UO}(t-1) + \phi_{32}\cdot M_{LO}(t-1), \tag{10}$$

$$M_{LO}(t) = \phi_{23}\cdot M_{UO}(t-1) + \phi_{33}\cdot M_{LO}(t-1). \tag{11}$$

The atmospheric concentration $M_{AT}(t)$ is composed of the current emissions, the share of the concentration remaining from the previous period plus the share of the upper oceanic concentration from the previous period that diffuses into the atmosphere. The upper oceanic concentration $M_{UO}(t)$ consists of the remaining share from the previous period plus the absorptions from the atmosphere and the lower oceans. The concentration in the lower oceans $M_{LO}(t)$ is

the remaining share of the previous period plus the absorption from the upper oceans. The parameters ϕ_{ij} control these relationships between different reservoirs and periods.

In the next step, the atmospheric carbon concentration $M_{AT}(t)$ increases the radiative forcing from the sun F(t) represented by:

$$F(t) = \eta \cdot \frac{M_{AT}(t)}{M_{AT}(preind)} + F_{exog}(t) \tag{12}$$

with η being a parameter that controls the impact of increasing greenhouse gas concentrations and $M_{AT}(preind)$ indicating the pre-industrial level of these concentrations. The term $F_{exog}(t)$ covers the additional radiative forcing caused by other greenhouse gases or aerosols that are exogenous in the model.

Finally, the increasing radiative forcing results in an increase of temperatures in the atmosphere $\Delta T_{AT}(t)$ as well as in the oceans $\Delta T_O(t)$ as given by equations (13) and (14):

$$\Delta T_{AT}(t) = \Delta T_{AT}(t-1) + \omega_1\left[F(t) - \omega_2 \Delta T_{AT}(t-1) - \omega_3\left(\Delta T_{AT}(t-1) - \Delta T_O(t-1)\right)\right], \tag{13}$$

$$\Delta T_O(t) = \Delta T_O(t-1) + \omega_4\left[\Delta T_{AT}(t-1) - \Delta T_O(t-1)\right]. \tag{14}$$

The change in atmospheric temperatures according to (13) results from the change of the previous period as well as from the current radiative forcing that is corrected for the previous period and the interference between atmosphere and oceans. Analogously, the temperature change in the oceans according to (14) is computed from the change of the previous period that is corrected for the interference between the oceans and the atmosphere. These relationships between radiative forcing and the temperature in different carbon reservoirs or different periods, respectively, are controlled by the parameters ω_i.